Diabetes, Metabolic Syndrome and Obesity

Dovepress
Taylor & Francis Group

Open Access Full Text Article

ORIGINAL RESEARCH

Multi-Radiomics Features of Super-Resolution MRI for Predicting Minor Amputation in Wagner 3 Diabetic Foot Ulcers

Bin Cao[1,2,*], Jiali Zhong[3,*], Jie Zhang[4], Dong Zhao[1,2]

[1]Center for Endocrine Metabolism and Immune Diseases, Beijing Luhe Hospital, Capital Medical University, Beijing, People's Republic of China; [2]Beijing Key Laboratory of Diabetes Research and Care, Beijing, 101149, People's Republic of China; [3]Department of Medical Imaging, Beijing Luhe Hospital, Capital Medical University, Beijing, People's Republic of China; [4]Department of Vascular Surgery, Beijing Luhe Hospital, Capital Medical University, Beijing, People's Republic of China

*These authors contributed equally to this work

Correspondence: Dong Zhao; Jie Zhang, Email zhaodong@ccmu.edu.cn; Zhangjiesjz@vip.163.com

Aim: This study aimed to investigate effectiveness of multi-radiomics features (RFs) extracted from super-resolution MRI for predicting minor amputation in patients with Wagner 3 diabetic foot ulcers.

Methods: 275 eligible patients with Wagner 3 ulcers were retrospectively included and randomly divided into a training set (n = 192) and a test set (n = 83). A deep-transfer learning network was utilized to process coronal proton density weighted images (PDWI) and generate super-resolution PDWI (SRPDWI). RFs were extracted separately from soft tissues and phalanges. Random forest models were then developed to predict minor amputation.

Results: The minor amputation rate was 36.4% for the left foot and 32.2% for the right foot. All random forest models demonstrated excellent performance in the training set, achieving AUC ranging from 0.91 to 0.99. In the test set, the integrated radiomics model (combining RFs extracted from both soft tissue and phalanges) exhibited superior performance, with an AUC of 0.83, sensitivity of 0.71, and specificity of 0.79. Additionally, the inclusion of clinical indicators did not enhance the predictive performance of the integrated radiomics model.

Conclusion: The multi-RFs extracted from SRPDWI demonstrated promising potential in predicting the risk of minor amputation for Wagner 3 diabetic foot ulcers.

Keywords: diabetic foot ulcer, super-resolution, radiomics, minor amputation

Introduction

Diabetic foot ulcers (DFU), commonly precipitated by infections, peripheral vascular disease, or neuropathy, present a significant health challenge, exacerbating morbidity and mortality rates in diabetic populations.[1,2] Approximately 18.6 million people worldwide are affected by DFU, with a lifetime prevalence estimated to range from 19% to 34% among individuals with diabetes.[3,4] According to the International Working Group on the Diabetic Foot, foot amputations are performed worldwide at a rate of one every 20 seconds, affecting more than 1 million individuals annually.[5] The Wagner classification is a commonly used grading system for DFU. Among them, Wagner 3 represents a particular state, typically not accompanied by necrosis but frequently exhibiting concurrent local abscesses and osteomyelitis.[6] Simultaneously, this grade poses the risks of amputation[7] and multidrug-resistant bacterial infections,[8] as well as rapid infection progression, necessitating prompt and decisive clinical decision-making regarding the necessity of amputation.

Magnetic resonance imaging (MRI), recognized for its exceptional contrast resolution and detailed anatomical depiction, is ideally suited for staging the extent of infection, which is extremely useful for guiding therapy of diabetic foot infection.[9] Radiomics shows potential in detecting subtle differences in intensity and texture within medical images, facilitating the direct analysis of tissue features from raw data.[10] Radiomics features (RFs) have demonstrated efficacy in

https://doi.org/10.2147/DMSO.S565938
Received: 24 September 2025
Accepted: 14 January 2026
Published: 10 February 2026

identifying osteomyelitis in DFU and periprosthetic joint infections,[11,12] both of which are closely associated with the risk of amputation in DFU. Hence, MRI-based radiomics holds promise in evaluating the risk of amputation in DFU. However, the precise application of radiomics on DFU relies on obtaining high-quality medical images.

Recent advances in super-resolution (SR) imaging, driven by deep learning, have significantly improved the resolution and clarity of medical images.[13] SR enhances image details, overcoming the limitations of conventional methods, especially in low-resolution or noisy clinical images. This allows for the extraction of more accurate and reproducible RFs, which are crucial for reliable clinical assessment.[14,15] Moreover, studies have shown that SR-derived RFs outperform those from original images in various diagnostic tasks,[16,17] further highlighting their potential value in the assessment of DFU complications.

Although MRI-based radiomics shows promise in assessing diabetic foot infections, its potential to predict amputation risk remains underexplored. This study aims to address this gap by evaluating the ability of SR MRI-derived radiomics to predict minor amputation risk in patients with Wagner 3 DFU.

Materials and Methods

Patients

This study was designed as a retrospective study. This study used previously collected data from patients with available MRI data, clinical characteristics, and follow-up information, who had consented for their data to be used in future research and had been treated at Beijing Luhe Hospital between November 2016 and September 2023.

The MRI datasets were retrospectively retrieved from the hospital's imaging system, and the corresponding clinical information was obtained from its Electronic Medical Record System.

Treatment was uniformly administered by the same diabetic foot treatment team. To minimize heterogeneity, our study specifically focused on toe ulcers, which represent over half of all DFUs.[18] In this study, minor amputation was defined as the amputation at the level of the toe. Written informed consent had previously been acquired from all participating individuals. This study was approved by the Institutional Review Board of Luhe Hospital, Capital Medical University (2024-LHKY-161-01) and conducted in accordance with the principles of the Declaration of Helsinki.

The inclusion criteria for this study included patients who met the following criteria: (1) diagnosis of type 2 diabetes according to the World Health Organization (WHO) guidelines;[19] (2) classified as Wagner Grade 3; and (3) had ulcers localized on the toes, including the dorsal aspect, interdigital spaces, and plantar aspect.

The exclusion criteria were as follows: (1) prior debridement or minor amputation before the MRI examination (n = 67); (2) absence of an MRI examination (n = 58); (3) Ankle-Brachial Index (ABI) < 0.8 (n = 44); (4) patient refusal of treatment at our center or loss to follow-up (n = 22); (5) inadequate MRI quality (n = 6). Ultimately, 275 diabetic patients were included in the study, and these patients with diabetes were randomly assigned to a training group (n = 192) and a test group (n = 83) in a 7:3 ratio. A schematic diagram illustrating the inclusion and exclusion criteria, as well as the research process of this study, is presented in Figure 1

MRI Protocol

All participants had undergone MRI examinations using a 3.0T MRI scanner (uMR780 3.0T, UIH, China). Each participant had been positioned supine for scanning, and an 18- or 24-channel head/neck combined coil had been utilized. Coronal proton density weighted imaging (PDWI) had been conducted with the following parameters: repetition time of 4000 ms, echo time of 42 ms, slice thickness of 4 mm with a slice spacing of 1 mm, acquisition matrix of 384 × 268, and field of view of 160×160 mm.

Extraction of RFs

DICOM-format images were acquired through the Picture Archiving and Communication System (Hinacom, Beijing, China). For subsequent analysis, only PDWI were used; other sequences were excluded.

Super-resolution reconstruction was performed using the OnekeyAI platform, which employs a deep transfer learning algorithm to enhance the in-plane resolution of PDWI images (original PDWI shown in Figure 2A). Specifically, the

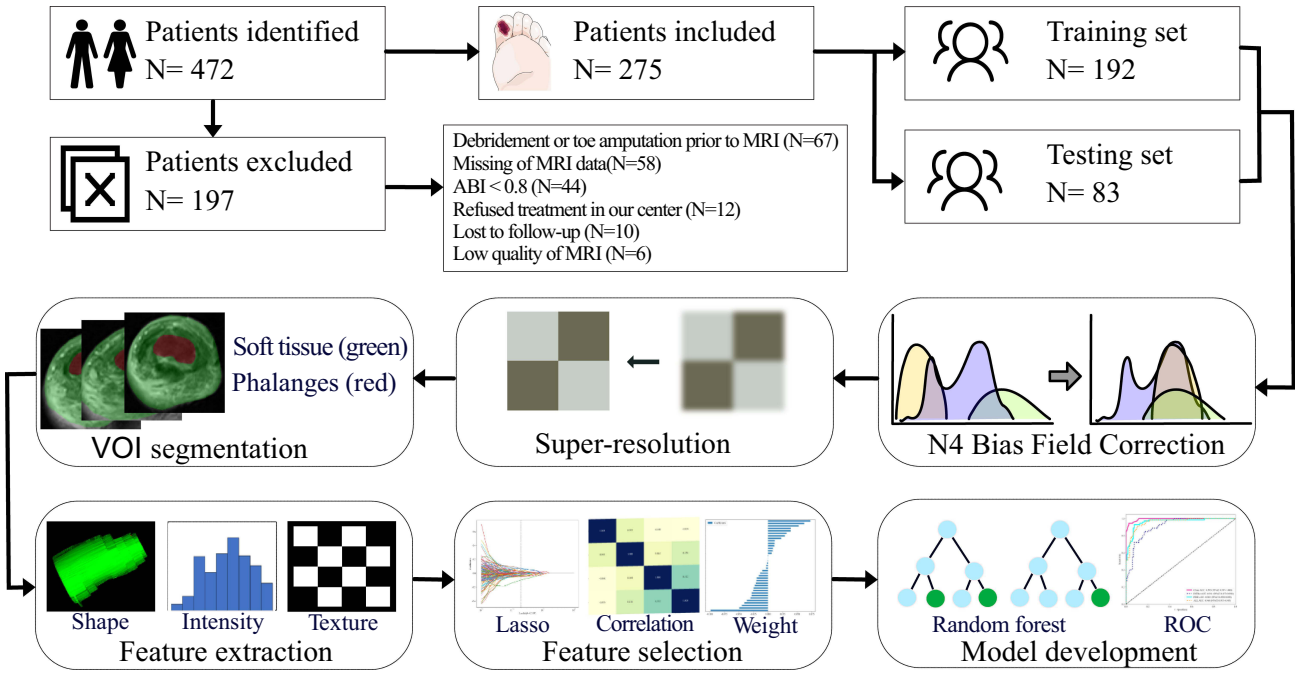

Figure 1 The schematic diagram of the model development flowchart. We collected the preoperative MRI images from eligible patients, performed a series of imaging processing, including N4 Bias Field Correction, super-resolution, and VOI outlining for different regions. After the radiomic features were extracted, we used LASSO regression to select robust features for further model development.

algorithm enhances both the x- and y-axis resolution of the images, reducing the voxel spacing from 0.312 × 0.312 × 5.000 mm to 0.156 × 0.156 × 5.000 mm, thereby generating super-resolution PDWI (SRPDWI) (Figure 2B). Structural similarity and normalized root mean square error were employed to evaluate image consistency before and after processing, yielding scores of 0.959 and 0.072, respectively. These results indicate minimal structural or intensity alterations alongside a marked improvement in spatial resolution. Finally, the volume of interest (VOI) corresponding to the infected toe was segmented on the SRPDWI.

Owing to the distinct tissue composition, the VOI was segmented into three subregions: the phalangeal VOI (Figure 2C), the soft tissue VOI (Figure 2D), and an integrated VOI encompassing both tissue types (Figure 2E). Delineation of all VOIs was performed manually in ITK-SNAP (open-source software; www.itk-snap.org) by two diabetic foot specialists, each possessing over five years of experience in MRI interpretation for diabetic foot disorders. To address segmentation reproducibility, we added a quantitative evaluation of inter-observer agreement. The Dice similarity coefficient between the two specialists was 0.90, indicating excellent consistency. Any inter-observer discrepancies were adjudicated through consensus. For each patient, RFs were independently extracted from the soft tissue and phalangeal subregions using the "PyRadiomics" package (version 3.0.1) in Python. The RFs derived from SRPDWI were categorized into three groups: geometric, intensity-based, and textural features. Geometric features quantify three-dimensional morphological characteristics, intensity features describe the statistical distribution of voxel values, and texture features capture spatial patterns of intensity heterogeneity through Gray-Level Co-occurrence Matrix (GLCM), Gray-Level Dependence Matrix (GLDM), Gray-Level Run-Length Matrix (GLRLM), Gray-Level Size Zone Matrix (GLSZM), and Neighborhood Gray-Tone Difference Matrix (NGTDM) analyses.

Features Selection and Models Construction

Feature selection and model construction were performed exclusively within the training set to prevent data leakage. For the RFs, we conducted *T*-test analysis for all features. Subsequently, only those features with a significance level of $p < 0.05$ were retained. To assess the correlation among features, we employed the Pearson correlation coefficient, and when the correlation coefficient between any two features larger than 0.9, only one feature was retained. We further selected

https://doi.org/10.2147/DMSO.S565938

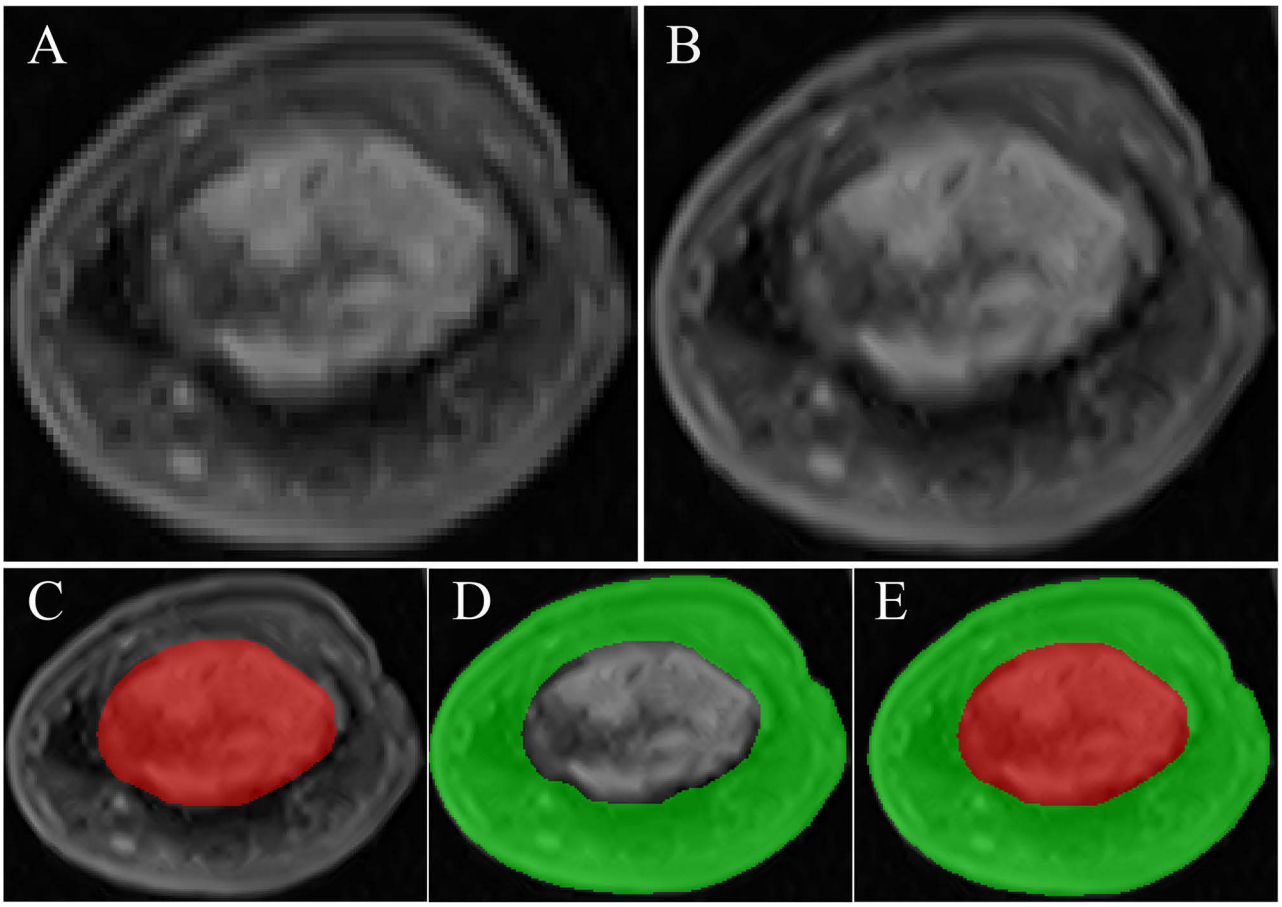

Figure 2 Diagram of super-resolution reconstruction and volume of interest (VOI) delineation. Initially, original coronal PDWI images (**A**) were downscaled for processing efficiency. Subsequently, a Generative Adversarial Network (GAN) was trained using paired low-resolution (LR) and synthetic high-resolution (HR) images. After training, transfer learning was applied to upscale the coronal PDWI, resulting in SRPDWI (**B**) with a resolution four times higher than the original PDWI images. The VOI was segmented into phalanges VOI (**C**), soft tissue VOI (**D**), and integrated VOI (**E**).

variables and determined the weights of non-zero variables using the least absolute shrinkage and selection operator (LASSO) regression. LASSO regression was performed using the LassoCV function in scikit-learn (version 1.5.0), with 10-fold cross-validation to identify the optimal regularization parameter (alpha) based on the minimum mean squared error. We developed and validated five models using random forest classification: a clinical model, a soft tissue radiomics model, a phalanges radiomics model, an integrated radiomics model, and a clinical-integrated radiomics model. In the clinical model, we analyzed the following clinical factors: sex, age, duration of diabetes, current smoking or drinking status, HbA1c level, white blood cell (WBC) counts, neutrophil percentage, estimated glomerular filtration rate (eGFR), and history of hypertension, coronary artery disease, and cerebral infarction. For the soft tissue radiomics model, the phalanges radiomics model, and the integrated radiomics model, only RFs were included in the analysis. In the clinical-integrated radiomics model, both the clinical risk factors and RFs were included in the analysis.

Following feature selection, random forest classification models were constructed using scikit-learn (version 1.0.2). The grid search algorithm was applied during model training, with 10-fold cross-validation implemented to determine optimal parameters and mitigate overfitting. We subsequently evaluated the performance of the five prediction models by plotting receiver operating characteristic (ROC) curves and calculating relevant metrics, including the area under the curve (AUC), sensitivity, specificity, positive predictive value, and negative predictive value. Furthermore, the clinical utility of each model was assessed via decision curve analysis (DCA), which quantified net benefits across a range of threshold probabilities.

Statistical Analysis

The Kruskal–Wallis test was utilized to validate differences in variables, while the chi-square test was employed to assess differences in composition ratios among groups. Statistical analyses were conducted using R software (version 4.3.2) and Python (version 3.7.12), with a significance threshold set at $P < 0.05$ for all two-sided tests.

Results

Clinical Characteristics

A total of 275 patients were included in the final analysis, with clinical data presented in Table 1. The mean age of the patients was 63.68 ± 12.12 years, with a mean duration of 14.24 ± 7.79 years. The average HbA1c level was 9.47 ± 2.08%. Males accounted for 58.91% of the cohort. 93 patients underwent minor amputation, while 182 ulcers healed. Patients who underwent minor amputation had longer diabetes duration, higher HbA1c levels, elevated WBC counts and neutrophil percentage, and lower albumin levels compared to the healed group. Additionally, their eGFR levels were lower, although not statistically significant. The incidence of ulcerations on each foot was higher on the first toe, with 35.7% on the left and 33.6% on the right (Figure 3A). The overall minor amputation rate was 36.4% for the left foot and 32.2% for the right foot (Figure 3B).

Development of Models for Minor Amputation Prediction

For each patient, we extracted a total of 3668 RFs (1834 RFs for soft tissue and phalanges, respectively), comprising 720 first-order features, 28 shape features, and 2920 texture features. The texture features were further divided into 880 GLCM, 640 GLRLM, 560 GLDM, 640 GLSZM, and 200 NGTDM methods. LASSO regression was performed for soft tissue RFs (Supplement Figure 1A), phalanges RFs (Supplement Figure 1B) and integrated RFs (Supplement Figure 1C) in the training cohort. Subsequently, the soft tissue RFs retained 29 non-zero features (Supplement Figure 2A), while the phalanges RFs retained 37 non-zero features (Supplement Figure 2B). Figure 4A illustrates 44 non-zero features of the integrated RFs, with 17 RFs originating from soft tissues and 27 RFs from phalanges.

For all five models, AUC and DCA were evaluated on the training set. Each model exhibited outstanding predictive performance, with AUC values ranging from 0.91 to 0.99 (Figure 4B). The DCA curves for all models consistently exceeded the two reference lines across threshold probabilities, demonstrating robust clinical utility (Figure 4C).

Table 1 Characteristics of Patients

	All (n= 275)	Healed (n= 182)	Toe Amputation (n= 93)	P value
Age (years)	63.68±12.12	63.57±12.45	63.90±11.51	0.830
Duration of diabetes (years)	14.24±7.79	13.37±7.75	15.95±7.62	0.009
Male (n, %)	162 (58.91)	108 (59.34)	54 (58.06)	0.941
Current smoker (n, %)	58 (21.09)	43 (23.63)	15 (16.13)	0.199
Current drinker (n, %)	34 (12.36)	26 (14.29)	8 (8.60)	0.246
Hypertension (n, %)	157 (57.09)	101 (55.49)	56 (60.22)	0.536
CHD (n, %)	79 (28.73)	50 (27.47)	29 (31.18)	0.615
Laboratory test				
HbA1c (%)	9.5±2.1	9.3±2.0	9.8±2.2	0.044
eGFR (mL/min per 1.73m2)	76.67±27.79	78.95±27.45	72.21±28.06	0.063
Bun (mmol/L)	6.81±3.70	6.45±3.41	7.51±4.12	0.056
Leukocyte (×109/L)	7.44±2.24	6.95±1.95	8.41±2.46	<0.001
Neutrophil (%)	69.27±9.19	67.70±9.35	72.34±8.06	<0.001
Albumin (g/L)	38.16±4.32	38.74±4.09	37.04±4.56	0.001

Abbreviations: eGFR, estimated glomerular filtration rate; BUN, blood urea nitrogen; CHD, coronary heart disease.

https://doi.org/10.2147/DMSO.S565938

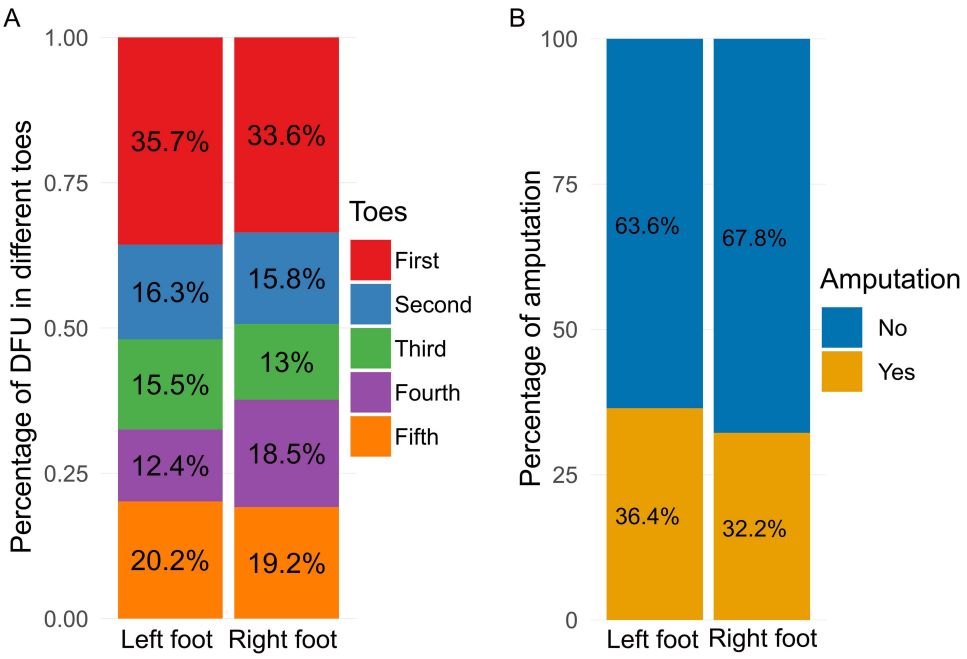

Figure 3 Distribution of ulcers on the toes of each foot (**A**), and probability of minor amputation for each foot (**B**).

Validation of Radiomic Models for Minor Amputation Prediction

Table 2 summarizes the AUC, sensitivity, specificity, positive predictive value (PPV), and negative predictive value (NPV) of the test set across the evaluated models. The clinical model yielded an AUC of only 0.48, reflecting poor predictive ability and significant overfitting. Both the soft tissue radiomics model and the phalanges radiomics model showed satisfactory overall performance, with the former achieving higher sensitivity and the latter demonstrating superior specificity. The integrated radiomics model emerged as the top performer, attaining the highest AUC along with competitively high sensitivity and specificity. Interestingly, the clinical-integrated radiomics model, which combines clinical variables with RFs, exhibited a decline in predictive performance compared to the integrated radiomics model alone.

The integrated radiomics model was identified as the final predictive model and subsequently validated on the test set. DCA demonstrated robust clinical utility, with the model's curve exceeding both reference lines across a wide range of threshold probabilities (Figure 5A). Using predicted probabilities from the model, patients were categorized into quartiles. A clear gradient in amputation risk was observed across these groups: the actual amputation rate was 0% in the first quartile and increased progressively to 69.2% in the fourth quartile (Figure 5B).

Discussion

Currently, decisions on whether amputation is necessary for DFU depend heavily on physicians' expertise and clinical experience, owing to the scarcity of high-quality clinical evidence to guide intervention strategies. The main goals of treatment are to prevent systemic infection, preserve as much healthy tissue as possible, and promote wound healing. In this study, we developed a set of robust random forest classifiers based on SRPDWI radiomics to predict minor amputation risk in patients with Wagner grade 3 toe ulcers. This approach shows potential for significantly reducing both clinical costs and diagnostic errors in the management of high-risk cases.

Radiomics has gained increasing traction in both oncology and bone research due to its capacity to extract clinically relevant texture features from medical images. For instance, MRI radiomics is useful for the diagnosis of breast lesions[20] and glioma,[21] while ultrasound radiomics contributes to the detection of endometrial cancer[22] and malignant thyroid nodules.[23] Similarly, the technique has shown considerable value in the field of bone disorders. Hirotaka Muraoka et al[24] employed MRI texture analysis to quantitatively assess acute osteomyelitis in the mandible, identifying significant differences in texture features between affected and healthy individuals. In another study, Michail E Klontzas et al[25]

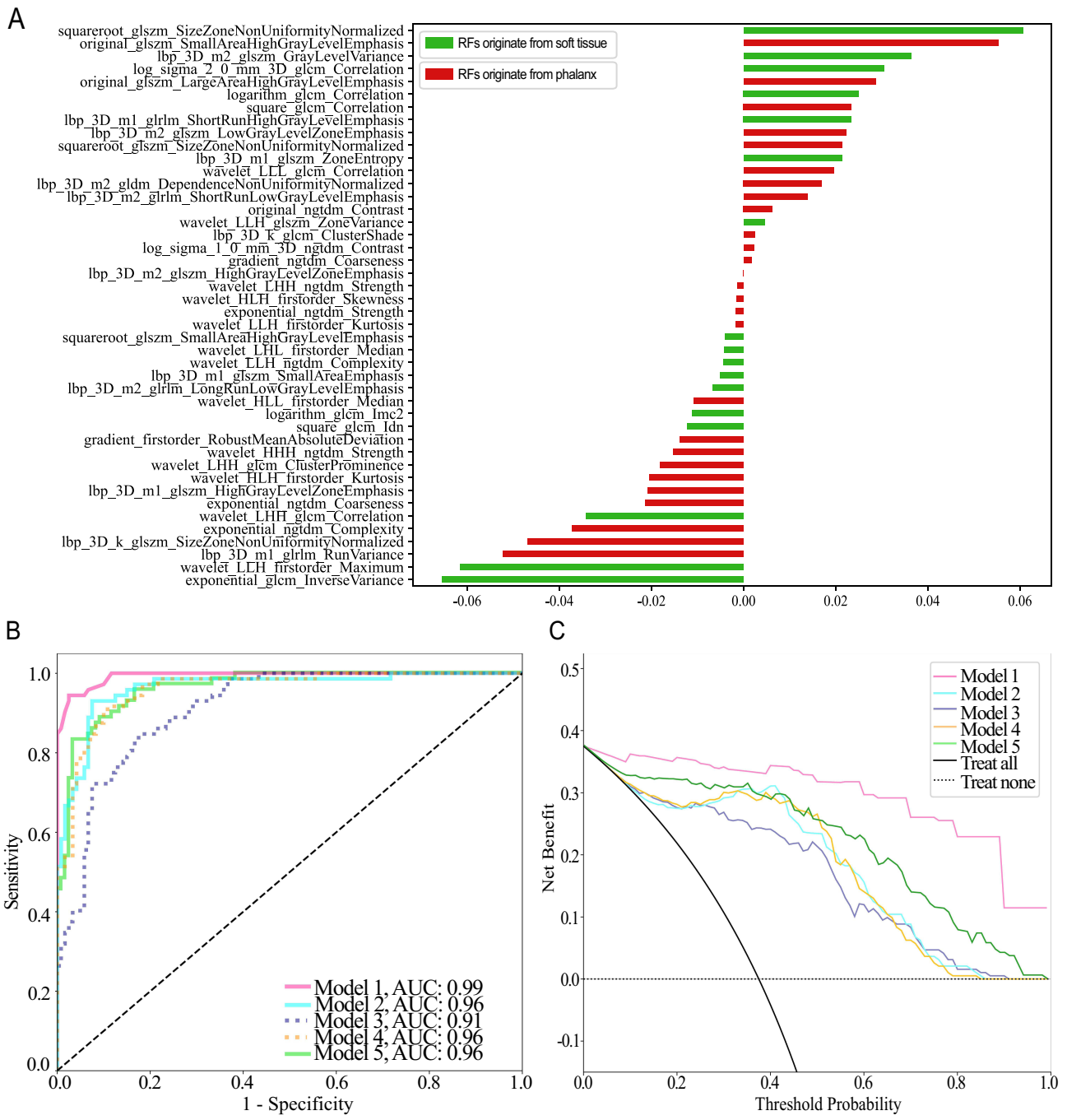

Figure 4 The histogram of the RFs importance score based on the integrated RFs (**A**). Receiver operating characteristic (ROC) curves (**B**) and DCA plot (**C**) for the five model in the training set.

extract MRI-based RFs from cases of transient osteoporosis and avascular necrosis. Their approach effectively distinguished between transient osteoporosis and avascular necrosis of the hip, underscoring the versatility and precision of radiomics in diagnosing intricate bone pathologies.

Although radiomics applications in diabetic foot are limited, emerging studies demonstrate its potential. Wang et al[11] reported that radiomics-based unsupervised clustering analysis can effectively distinguish periprosthetic hip joint infections. Ferhat Cuce et al[12] utilized radiomics to differentiate bone marrow signal abnormalities in diabetic foot, focusing on conditions such as Charcot neuroarthropathy and osteomyelitis. Likewise, the utilization of radiomics in the context of skin infections has not been well-documented in the literature. However, it is encouraging that radiomics

https://doi.org/10.2147/DMSO.S565938

Table 2 Performance of All Models

	Model 1	Model 2	Model 3	Model 4	Model 5
AUC (95% CI)	0.48 (0.32–0.63)	0.71 (0.58–0.85)	0.77 (0.64–0.90)	0.83 (0.73–0.93)	0.76 (0.65–0.87)
SEN	0.24	0.76	0.57	0.71	0.76
SPE	0.76	0.55	0.89	0.79	0.68
PPV	0.25	0.36	0.63	0.54	0.44
NPV	0.75	0.87	0.86	0.89	0.89

Notes: Model 1 clinical model. Model 2 soft tissue radiomics model. Model 3 phalanges radiomics model. Model 4 integrated radiomics model. Model 5 clinical factors-integrated radiomics model.
Abbreviations: AUC, area under curve; 95% CI, 95% confidence interval; SEN, sensitivity; SPE, specificity; PPV, positive predictive value; NPV, negative predictive value.

technology has already been utilized in studies related to radiation-induced dermatitis.[26,27] These studies illustrated the capacity of radiomics to identify skin and bone-joint related inflammatory lesions. Osteomyelitis occurs almost exclusively by the contiguous spread of infection to the bone from adjacent skin ulceration.[28] In Wagner 3 ulcers, the infection penetrates deep tissues, often result in osteomyelitis. A comprehensive consideration of the impact of infection on the phalanges and peripheral soft tissues is essential for the assessment of the risk of amputation. In the present study, we extracted VOI from phalanges and skin soft tissues separately and harvested RFs. Our research found that the specificity of RFs extracted from the phalanges reached up to 88.7%, but its sensitivity was insufficient. In contrast, RFs extracted from soft tissues exhibited a higher sensitivity of 76.2% but a lower specificity. Therefore, we combined the modeling of RFs extracted from both the phalanges and soft tissues. The integrated model combined the strengths of both independent models, achieving both good sensitivity (71.4%) and specificity (79.0%). The results suggest that these RFs hold significant predictive value for determining the need for minor amputation.

Commonly identified risk factors for amputation in DFU include duration of diabetes, poor glycemic control, albumin, and infection.[29,30] According to recent data, a longer duration of diabetes is associated with an increased risk of DFU.[31] A possible explanation is that a longer duration of diabetes is associated with a higher rate of microvascular and macrovascular complications such as peripheral neuropathy, and cumulative effects of poor glycemic control.[4] Chronic hyperglycemia cause a stress response and induce immune disorders, disrupts wound healing.[32] In clinical

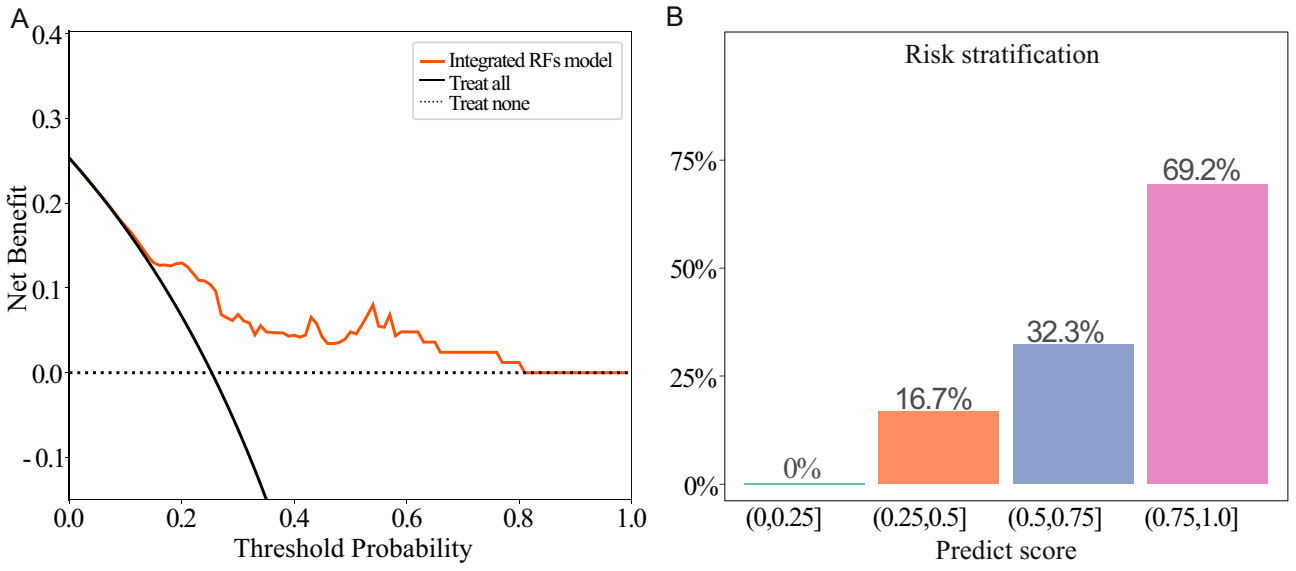

Figure 5 The predict score of random forest for each patient in the test set (**A**). Risk stratification based on the predict score, the patients were divided into quartiles, and the amputation rate escalated progressively among the groups as the predicted risk escalated (**B**).

https://doi.org/10.2147/DMSO.S565938

practice, WBC count and neutrophil count are commonly used parameters for detecting infection in DFUs, and they are indicative of the risk of amputation.[33,34] The study also included clinical data such as duration of diabetes, glycemic indicators (glycated hemoglobin), infection indicators (WBC and neutrophils), and albumin levels to construct a predictive model. However, the results indicated that the prediction model based solely on clinical indicators suffered from severe overfitting, and incorporating these indicators into the radiomic features did not improve the prediction performance. DFU present complex conditions with significant individual variations. While our study also indicated that the aforementioned indicators are indeed risk factors for amputation, relying solely on clinical indicators for the precise prediction of minor amputation proves to be inaccurate.

This study has several limitations. Firstly, we chose to utilize the 2D PDWI sequence instead of the 3D PDWI sequence. While 3D PDWI sequences theoretically offer superior three-dimensional information and are more conducive to image feature extraction, they typically require longer examination times and necessitate the feet to remain stationary during MRI, posing challenges for patients with foot infections. Another limitation is that we only included non-ischemic diabetic foot cases. This decision was made to maintain a more uniform patient group, but it restricts the broader applicability of the findings. We also acknowledge that both overfitting and the high feature-to-event ratio remain key concerns for model validation. These results should be viewed as a proof-of-concept, rather than as a definitive, ready-for-clinical-use tool. Future studies must include a more diverse cohort and undergo prospective, multicenter validation before clinical adoption. Besides, the process of manual segmentation of the volume of interest (VOI) also poses challenges. Though experienced radiologists performed the segmentation and resolved any discrepancies through discussion, manual methods are time-consuming and can introduce variability. Future work should explore the use of automated or semi-automated segmentation methods to save time and increase consistency. Finally, as with most radiomics studies, interpretability remains a challenge. Developing clear and standardized methods to link radiomic features with biological processes in diabetic foot ulcers will help provide stronger insights and practical applications for these models in clinical settings.

In conclusion, this study showed that multi-RFs extracted from SRPDWI have promising potential for predicting minor amputation in patients with Wagner 3 DFUs. The integrated radiomics model performed best among all models. Notably, traditional clinical indicators did not enhance model performance. This suggests that, for this specific task, imaging-derived phenotypic features may provide more predictive value than routine laboratory markers. However, given the single-center and retrospective nature of this study and the potential risk of model overfitting, rigorous prospective multicenter validation is essential before this model can be considered for any clinical application.

Data Sharing Statement

The data that support the findings of this study are available from the corresponding author, upon reasonable request.

Acknowledgments

The authors thank all participants in the study, and extend special appreciation to Ling Zhang for her guidance and assistance in preparing this paper.

Author Contributions

Dong Zhao and Jie Zhang: Conceptualization, supervision and writing – review & editing. Bin Cao and Jiali Zhong: Data curation. Bin Cao and Jiali Zhong: Formal analysis and writing – original draft. All authors gave final approval of the version to be published; have agreed on the journal to which the article has been submitted; and agree to be accountable for all aspects of the work.

Funding

This study was funded by the Science and Technology Committee of Tongzhou District (Number: KJ2023CX034, KJ2024CX029, CXTD2024003).

Disclosure

The authors declare they have no conflict of interest.

References

1. Armstrong DG, Boulton AJM, Bus SA. Diabetic foot ulcers and their recurrence. *N Engl J Med*. 2017;376:2367–2375. doi:10.1056/NEJMra1615439
2. Alavi A, Sibbald RG, Mayer D, et al. Diabetic foot ulcers: Part I. Pathophysiology and prevention. *J Am Acad Dermatol*. 2014;70:1.e1–18; quiz 19–20. doi:10.1016/j.jaad.2013.06.055
3. Armstrong DG, Tan T-W, Boulton AJM, Bus SA. Diabetic foot ulcers: a review. *JAMA*. 2023;330:62. doi:10.1001/jama.2023.10578
4. McDermott K, Fang M, Boulton AJM, Selvin E, Hicks CW. Etiology, epidemiology, and disparities in the burden of diabetic foot ulcers. *Diabetes Care*. 2023;46:209–221. doi:10.2337/dci22-0043
5. Schaper NC, van Netten JJ, Apelqvist J, et al. Practical Guidelines on the prevention and management of diabetic foot disease (IWGDF 2019 update). *Diabetes Metab Res Rev*. 2020;36 Suppl 1:e3266. doi:10.1002/dmrr.3266
6. Lim JZM, Ng NSL, Thomas C. Prevention and treatment of diabetic foot ulcers. *J R Soc Med*. 2017;110:104–109. doi:10.1177/0141076816688346
7. Jeon B-J, Choi HJ, Kang JS, Tak MS, Park ES. Comparison of five systems of classification of diabetic foot ulcers and predictive factors for amputation. *Int Wound J*. 2017;14:537–545. doi:10.1111/iwj.12642
8. Chen T, Yu J, Ye J, et al. Infection characteristics and drug susceptibility of multidrug-resistant bacteria in patients with diabetic foot ulcers. *Clin Lab*. 2023;69. doi:10.7754/Clin.Lab.2023.230309
9. Lipsky BA, Berendt AR, Deery HG, et al. Diagnosis and treatment of diabetic foot infections. *Plast Reconstr Surg*. 2006;117:212S–238S. doi:10.1097/01.prs.0000222737.09322.77
10. Mayerhoefer ME, Materka A, Langs G, et al. Introduction to radiomics. *J Nucl Med*. 2020;61:488–495. doi:10.2967/jnumed.118.222893
11. Wang Y, Wang R, Zhang X, et al. Diagnostic efficiency of [68 Ga]Ga-DOTA-FAPI-04 in differentiating periprosthetic Hip joint infection and aseptic failure. *Eur J Nucl Med Mol Imaging*. 2023;50:1919–1928. doi:10.1007/s00259-023-06146-y
12. Cuce F, Tulum G, Yılmaz KB, Osman O, Aralasmak A. Radiomics method in the differential diagnosis of diabetic foot osteomyelitis and charcot neuroarthropathy. *Br J Radiol*. 2023;96:20220758. doi:10.1259/bjr.20220758
13. Niaz MR, Ridwan AR, Wu Y, et al. Development and evaluation of a high resolution 0.5mm isotropic T1-weighted template of the older adult brain. *Neuroimage*. 2022;248:118869. doi:10.1016/j.neuroimage.2021.118869
14. Park S, Lee SM, Do K-H, et al. Deep learning algorithm for reducing CT slice thickness: effect on reproducibility of radiomic features in lung cancer. *Korean J Radiol*. 2019;20:1431–1440. doi:10.3348/kjr.2019.0212
15. de Farias EC, Di Noia C, Han C, et al. Impact of GAN-based lesion-focused medical image super-resolution on the robustness of radiomic features. *Sci Rep*. 2021;11:21361. doi:10.1038/s41598-021-00898-z
16. Fan M, Liu Z, Xu M, et al. Generative adversarial network-based super-resolution of diffusion-weighted imaging: application to tumour radiomics in breast cancer. *NMR Biomed*. 2020;33:e4345. doi:10.1002/nbm.4345
17. Hou M, Zhou L, Sun J. Deep-learning-based 3D super-resolution MRI radiomics model: superior predictive performance in preoperative T-staging of rectal cancer. *Eur Radiol*. 2023;33:1–10. doi:10.1007/s00330-022-08952-8
18. Pickwell KM, Siersma VD, Kars M, et al. Diabetic foot disease: impact of ulcer location on ulcer healing. *Diabetes Metab Res Rev*. 2013;29:377–383. doi:10.1002/dmrr.2400
19. Alberti KG, Zimmet PZ. Definition, diagnosis and classification of diabetes mellitus and its complications. Part 1: diagnosis and classification of diabetes mellitus provisional report of a WHO consultation. *Diabet Med*. 1998;15:539–553. doi:10.1002/(SICI)1096-9136(199807)15:7<539::AID-DIA668>3.0.CO;2-S
20. Jiang Y, Edwards AV, Newstead GM. Artificial Intelligence Applied to Breast MRI for Improved Diagnosis. *Radiology*. 2021;298:38–46. doi:10.1148/radiol.2020200292
21. Takahashi S, Takahashi W, Tanaka S, et al. Radiomics analysis for glioma malignancy evaluation using diffusion kurtosis and tensor imaging. *Int J Radiat Oncol Biol Phys*. 2019;105:784–791. doi:10.1016/j.ijrobp.2019.07.011
22. Moro F, Albanese M, Boldrini L, et al. Developing and validating ultrasound-based radiomics models for predicting high-risk endometrial cancer. *Ultrasound Obstet Gynecol*. 2022;60:256–268. doi:10.1002/uog.24805
23. Liang J, Huang X, Hu H, et al. Predicting malignancy in thyroid nodules: radiomics score versus 2017 American College of Radiology Thyroid Imaging, Reporting and Data System. *Thyroid*. 2018;28:1024–1033. doi:10.1089/thy.2017.0525
24. Muraoka H, Ito K, Hirahara N, et al. Magnetic resonance imaging texture analysis in the quantitative evaluation of acute osteomyelitis of the mandibular bone. *Dentomaxillofac Radiol*. 2022;51:20210321. doi:10.1259/dmfr.20210321
25. Klontzas ME, Manikis GC, Nikiforaki K, et al. Radiomics and machine learning can differentiate transient osteoporosis from avascular necrosis of the Hip. *Diagnostics*. 2021;11:1686. doi:10.3390/diagnostics11091686
26. Park S-Y, Park JM, Kim J-I, et al. Quantitative radiomics approach to assess acute radiation dermatitis in breast cancer patients. *PLoS One*. 2023;18:e0293071. doi:10.1371/journal.pone.0293071
27. Feng H, Wang H, Xu L, et al. Prediction of radiation-induced acute skin toxicity in breast cancer patients using data encapsulation screening and dose-gradient-based multi-region radiomics technique: a multicenter study. *Front Oncol*. 2022;12:1017435. doi:10.3389/fonc.2022.1017435
28. Ledermann HP, Morrison WB, Schweitzer ME. MR image analysis of pedal osteomyelitis: distribution, patterns of spread, and frequency of associated ulceration and septic arthritis. *Radiology*. 2002;223:747–755. doi:10.1148/radiol.2233011279
29. Zhu Y, Xu H, Wang Y, et al. Risk factor analysis for diabetic foot ulcer-related amputation including Controlling Nutritional Status score and neutrophil-to-lymphocyte ratio. *Int Wound J*. 2023;20:4050–4060. doi:10.1111/iwj.14296
30. Kang H, Choi S, Park Y-G, Choi J, Lim C. Risk factors for major lower limb amputation and effect of endovascular revascularization in patients with diabetic foot wound. *Indian J Orthop*. 2024;58:379–386. doi:10.1007/s43465-024-01100-y
31. Shao Z, Wang Z, Bi S, Zhang J. Establishment and validation of a nomogram for progression to diabetic foot ulcers in elderly diabetic patients. *Front Endocrinol*. 2023;14:1107830. doi:10.3389/fendo.2023.1107830
32. Godbout JP, Glaser R. Stress-induced immune dysregulation: implications for wound healing, infectious disease and cancer. *J Neuroimmune Pharmacol*. 2006;1:421–427. doi:10.1007/s11481-006-9036-0

33. Sun J-H, Tsai J-S, Huang C-H, et al. Risk factors for lower extremity amputation in diabetic foot disease categorized by Wagner classification. *Diabet Res Clin Pract*. 2012;95:358–363. doi:10.1016/j.diabres.2011.10.034
34. Sen P, Demirdal T, Emir B. Meta-analysis of risk factors for amputation in diabetic foot infections. *Diabetes Metab Res Rev*. 2019;35:e3165. doi:10.1002/dmrr.3165